Dynamic wavefront and polarisation control for ultrashort-pulse laser microprocessing

8th International Conference on
Photonic Technologies LANE 2014

Industrial Paper

Dynamic wavefront and polarisation control for ultrashort-pulse laser microprocessing

Stuart P. Edwardson[a,]*, Olivier Allegre[a], Yang Jin[a], Walter Perrie[a], Geoff Dearden[a]

[a]*University of Liverpool, Laser Group, School of Engineering, Liverpool, L69 3GH, UK*

- Invited Paper -

Abstract

New developments in wavefront and polarisation control for ultrashort-pulse laser microprocessing are presented. Two Spatial Light Modulators are used in combination to structure the optical fields of a picosecond-pulse laser beam, producing vortex wavefronts and radial or azimuthal polarisation states. Demonstration of multiple first-order beams with vortex wavefronts and radial or azimuthal polarization states is given, produced using Computer Generated Holograms. The beams produced are used to nano-structure a highly polished metal surface. Laser Induced Periodic Surface Structures are observed and used to directly verify the state of polarisation in the focal plane and help to characterize the optical properties of the setup.

Keywords: Laser micromachining; Ultra-short pulse; Polarisation; Wavefront; Control; Spatial Light Modulator; SLM; LIPPS

1. Introduction

Laser micromachining using ultrashort pulses with temporal pulse lengths <10ps minimises thermal diffusion, lowers ablation thresholds and can generate highly reproducible micro and nano-structures (Le Harzic et al 2005, Banks et al 1999, Breitling et al 2004). As a result, industrial processes based on femtosecond and picosecond laser pulse durations are becoming increasingly widespread. Manufacturing applications include the very precise drilling of holes for fuel-injection nozzles (Breitling et al 2004), the dicing of silicon wafers (Sudani et al 2009), the scribing of thin film solar cells (Račiukaitis et al 2013) and the fabrication of volume Bragg gratings in transparent bulk materials (Liu et al 2010). Early ultrashort-pulse laser systems suffered from a comparatively low processing speed which slowed down their uptake in industry. This has partly been addressed by the development of higher repetition laser systems from 200kHz to > 1MHz (Bellouard 2012). However as repetition rates increase above 200kHz, the required scan speeds from Galvo systems can be problematic, leading to a high pulse overlap where plasma absorption can produce wavefront distortions (Breitling et al 2004).

An additional route to increase process efficiency further is to structure the wavefront of the beam by the use of a fixed optic such as an axicon (Rioux et al 1978) or a Spatial Light Modulator (SLM) (Sanner et al 2007). For example, inducing a vortex structure to the beam wavefront (i.e. adding orbital angular momentum to the laser light) produces a ring-shaped focal spot which helps to reduce the recast formation that typically appears after laser pulse ablation (Hamazaki et al 2010, Duocastella et al 2012). Furthermore, structuring the beam wavefront with a Computer Generated Hologram (CGH) has also been used to produce multiple diffractive beams for high-speed parallel processing applications such as the manufacture of volume Bragg gratings (Liu et al 2010) and of three-dimensional micro patterns (Jenness et al 2008). This method can increase throughput by more than an order of magnitude compared with traditional single-beam processing Hayasaki et al 2005, Kuang et al 2009, Hasegawa et al 2013).

A greater flexibility for micromachining can also be achieved by controlling polarization. Polarization is a critical parameter in the linear and non-linear interaction of laser radiation with matter. For example, simple

* Corresponding author. Tel.: +44-151-794-4639 ; fax: +44-151-650-2305 .
E-mail address: s.p.edwardson@liverpool.ac.uk

Fresnel reflection from a dielectric interface near Brewster's angle (Fowles 1975), atomic absorption and emission of light in the presence of a magnetic field (Zeeman effect) (Kleinpoppen 1997) and ultrafast laser surface ablation (Guay et al 2012) all show significant effects of incident polarization state. In Guay et al 2012, the observed asymmetric ablation geometries and nano-structures were related to the direction of linear polarization. Also, high intensity non-linear phenomena such as self-focusing (Boyd 2008), filamentation (Braun et al 1995, Panov et al 2013) and multi-photon ionization (MPI) in atoms (Fox et al 1971, Kogan et al 1971), molecules (Carman et al 1989) and solids (Venable et al 1975, Temnov et al 2006)) are all polarization sensitive. With MPI at low nonlinear order N δ 4, circular polarization couples more strongly than linear (Fox et al 1971, Kogan et al 1971) while at high N ε 6 a significant reversal occurs, decisively demonstrated in the 6-photon MPI of fused silica and sapphire with near-infrared (NIR), 50fs laser pulses yielding ($\sigma_{6\ lin}/\ \sigma_{6\ circ}$) ~3.7 and ~7 respectively (Temnov et al 2006) in agreement with theoretical predictions (Reiss 1972). These differences arise from quantum selection rules, applicable even in solids and related to conservation of angular momentum during the absorption process.

Polarization is also known to affect the speed and quality of processes such as drilling (Allegre et al 2012, Nolte et al 1999) and surface structuring (Venkatakrishnan 2002). Circularly polarized beams are chosen for some laser processing applications due to their isotropic properties (Nolte et al 1999); however, they do not offer the best processing speed (Niziev et al 1999). Radially or azimuthally polarized beams were recently demonstrated to improve processing speed and quality (Weber et al 1999, Meier et al 2007, Venkatakrishnan et al 2006). Thanks to the latest developments in liquid-crystal SLM, it is now possible to simultaneously control both the wavefront and polarization of laser beams (Reiss 1972, Beversluis et al 2006, Qi et al 2013, Allegre et al 2012). This enables for example producing multiple diffractive beams, where neighbouring beams have mutually orthogonal linear polarization states (Hasegawa et al 2013). The use of two SLMs for laser processing with parallel vortex beams and parallel beams with a radial or azimuthal polarization state is a novel development by the authors (Allegre et al 2013, Jin et al 2013). This conference paper thus reviews a technique for ultrashort-pulse laser microprocessing with complete control of the beam wavefront and polarization, using two SLMs in combination.

2. Experimental

2.1. Experimental Set-up

A schematic of the experimental setup is shown in Fig. 1. The laser source is a Coherent Talisker with a pulse width of 10ps, a wavelength of 532nm (linewidth ~0.1nm), M^2 <1.3, average power of 8W, 200kHz maximum repetition rate and a horizontal linear polarization. The beam is expanded using a telescope (Jenoptic) with ×3 magnification. To modulate wavefront as well as polarization, two Hamamatsu X10468-04 LCOS-SLMs (Liquid-Crystal On Silicon Spatial Light Modulators) and a pair of zero-order waveplates are used (Fig. 1).

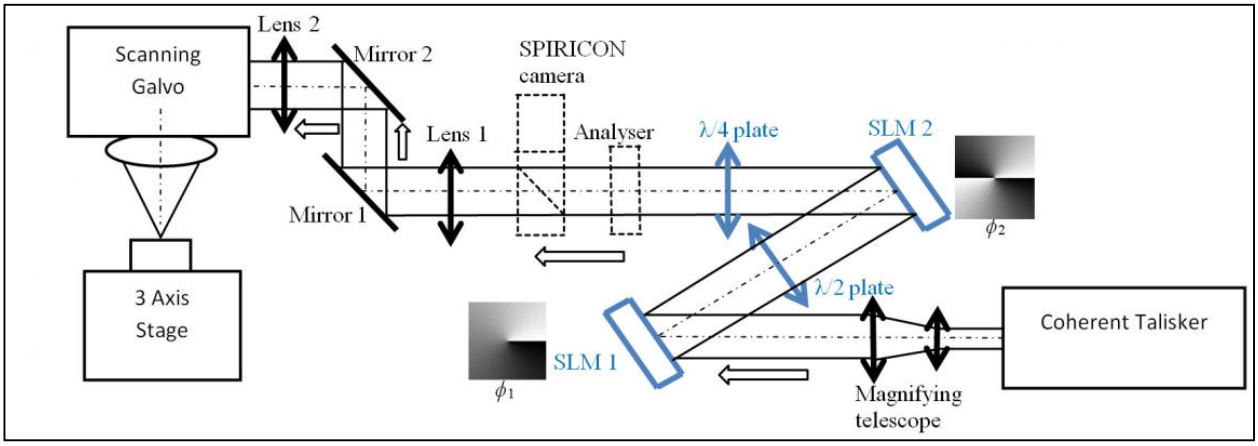

Fig. 1. Schematic showing how the SLMs together with the waveplates are used to control the wavefront and polarization of a picosecond-pulse laser microprocessing setup. The laser source provides a 532nm wavelength, 10ps pulse beam with a horizontal linear polarization, incident on SLM1. After SLM1, a half-waveplate tilts the polarization direction to + 45º, incident on SLM2. In this setup, SLM1 is used to control the wavefront whereas SLM2 is used to control the polarization. The "polarization test components" are removed when the microprocessing tests are carried out.

The SLMs (referred to as SLM1 and 2 in Fig. 1) are of the phase-only, reflection type and consist of a 16x12mm, 800x600 pixel array of horizontally oriented liquid-crystal phase retarders. SLM1 is used to control the wavefronts whereas SLM2, together with the waveplates, is used to control polarization.

After the SLMs, there is 4f optical system (Lens 1 and 2 in Fig. 1) which uses planoconvex lenses (f = 400mm) to re-image the surface of SLM2 (Fig. 1) to the 15mm input aperture of a scanning galvo (Nutfield). At the galvo output, the beam is focused with a flat field f-theta lens (f = 250mm). For processing experiments, samples are mounted on a precision 3-axis (x, y, z) motion control system (A3200 Ndrive system, Aerotech) allowing accurate positioning in the focal plane. The modulation of polarization is synchronized with the beam scanning motion on the sample thanks to a real-time control unit Aerotech Nmark SSam (Synchronized Scanning and motion) which runs within a Labview environment, driving the scanning galvo as well as synchronizing application of previously Computer- Generated phase Holograms (CGHs) to the SLMs.

Prior to processing the samples, the collimated beam is analyzed with a SPIRICON beam profiler and a polarizing filter located just before Lens 1 (see Fig. 1). The camera had no focusing lens.

2.2. Optical Configurations

If the arrays $\phi_1(x, y)$ and $\phi_2(x, y)$ are the relative phase delays, or CGHs, induced with the first and second SLM respectively (Fig. 1), the wavefront and polarization can be controlled by adjusting these two components respectively, so that the resulting beams have the desired optical field structures. For the experiments, the SLMs were configured to produce four distinct optical field configurations: linearly polarized beams (horizontal or vertical) with a vortex wavefront (carrying an orbital angular momentum of $l = 1$), or radially and azimuthally polarized beams with a planar wavefront.

The (fixed) CGH applied to SLM1 created a vortex wavefront whereas the four CGHs sequentially applied to SLM2 modulated the polarization states. All these optical field configurations produce the same ring-shaped intensity distribution when focused with a low NA lens such as the one used in the experiment. Therefore the fluence at the sample surface is the same in each case. Importantly, the SLMs enable the user to dynamically control the phase delays $\phi1(x, y)$ and $\phi2(x, y)$ so that the state of polarization can be modulated in real-time.

2.3. Experimental procedure

For the experiments, the modulated laser beam is used to process the surface of highly polished stainless steel samples, using a fluence near the ablation threshold of steel, which is ~0.16J/cm^2. This leads to the formation of wavelength-sized LIPSS, which develop orthogonally to the local electric field vectors of the beam. Therefore, by modulating the incident polarization field, we control the way LIPSS develop on the surface. The experiments consisted in laser processing the sample surface, whilst dynamically changing the polarization fields so as to produce the desired LIPSS patterns over large scales.

For all these tests, the laser output is attenuated to produce a pulse energy of 3μJ (fluence F ~0.2J/cm^2 at focal plane). Various processing geometries are used, where the sample is exposed to produce either sets of discrete laser spots or continuous scanned lines. In the former case each spot is exposed for 20ms whilst the beam remains static and in the latter case the beam is scanned at 2.5mm/s. In either case each region is exposed with an average pulse overlap of ~100pulses, with a pulse repetition rate of 5kHz. After laser exposure, the processed surfaces are imaged with an optical microscope and Scanning Electron Microscope (SEM).

3. Results and Discussion

Thanks to its flexibility, the setup allows processing a wide range of geometries, where the desired state of polarization is applied within each region. A number of experimental configurations are demonstrated below.

3.1. Discrete patterns of laser spots with polarization control

As a first case study, the experimental setup was configured to produce a discrete pattern of laser spots, where the overall geometry was designed to represent four letters “LLEC” (Fig. 2, representing Lairdside Laser Engineering Centre), each with a distinct state of polarization. Thus, four sets of laser spots are sequentially produced so that each letter of the geometry has a different state of polarization. Each spot was imprinted with 100 pulses at 0.2J/cm2 (see processing parameters in Section 2.3 above) and the overall exposure duration for the whole geometry was ~4s (52spots) corresponding to a polarization switching bandwidth of ~1Hz.

The bandwidth of polarization switching was calculated approximately from the time taken to micro-structure the overall pattern, allowing for the number of switching cycles during the procedure (with nearly the same number of spots in each letter). After laser processing, a microscopic investigation of the produced geometry revealed the details of the laser spots (Fig. 2). As expected, each produced laser spot had a ring-shaped structure. The laser exposure had also led to the development of LIPSS within each spot. The geometry of LIPSS, imaged with an SEM in Fig. 2, is consistent with that expected when processing with a linear, radial or azimuthal state of

polarization. Note that the micro-machined spots do show some residual distortion in their shape due to the resolution limit of the SLMs, where the pixel size (~20μm) and discrete phase modulation induced some discontinuity in the produced wavefronts which affected the focal intensity distributions.

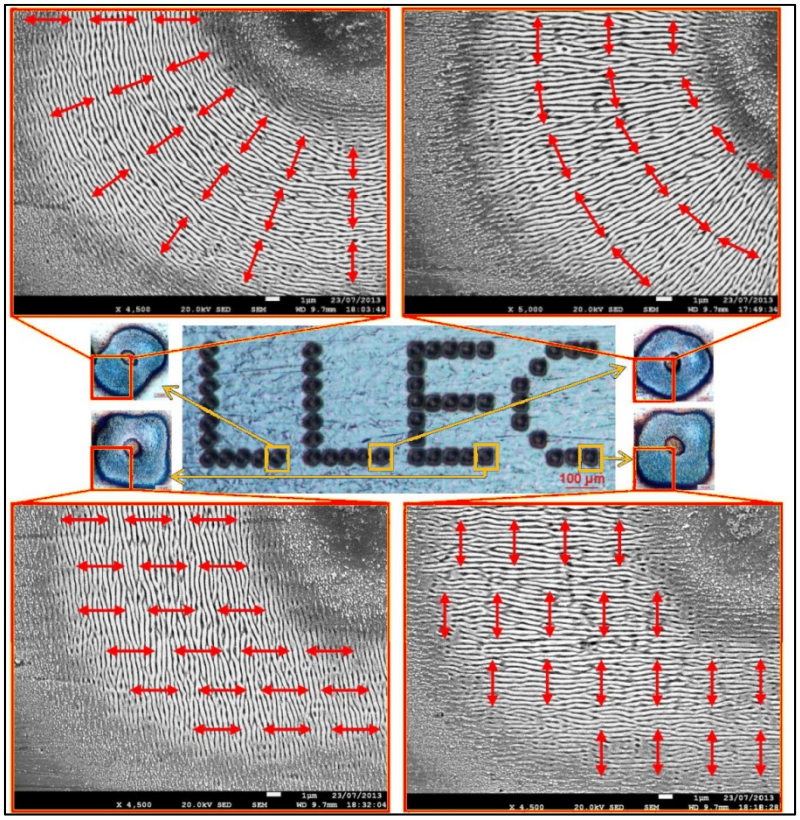

Fig. 2. (Centre) Optical micrographs showing the processed geometry, which is produced by marking four distinct sets of laser spots, each set using a different state of polarization. (Top and bottom) magnified regions of laser spots, imaged with an SEM. The ablation spots had been produced either with a radially (top-left inlay), azimuthally (top-right inlay), horizontally (bottom-left) and vertically (bottom-right) polarized beam. The red arrows represent the direction of local electric field vectors.

3.2. Continuous linear scanning with synchronized dynamic polarization control

The states of polarization can be easily modulated in real-time during processing. Complex two dimensional patterns of LIPSS can be produced using linear scanning with dynamic control of polarization (Fig 3.). The setup was configured to scan along a raster pattern, where polarization was sequentially changed during scanning. The state of polarization was synchronized with the beam scanning motion so as to produce the desired pattern of LIPSS in each region of the scanned geometry. The processing parameters are described in Section 2.3 above. Fig 3 shows optical micrographs of the produced figures and confirms that synchronization is complete. The microscopic analysis confirmed that the expected, complex LIPSS patterns had been produced in each region with polarizations switched synchronously at $\nu = 12.5$Hz.

The polarization states are easily visualized using low-angle side illumination shown in the optical micrographs in Fig. 3 where two illumination sources (white light, unpolarized) at grazing incidence were used, located on either side of the sample along a single axis (blue arrows in Fig. 3). Due to their diffractive properties, only the areas where LIPSS are perpendicular to the axis of illumination reflected the low-angle light,

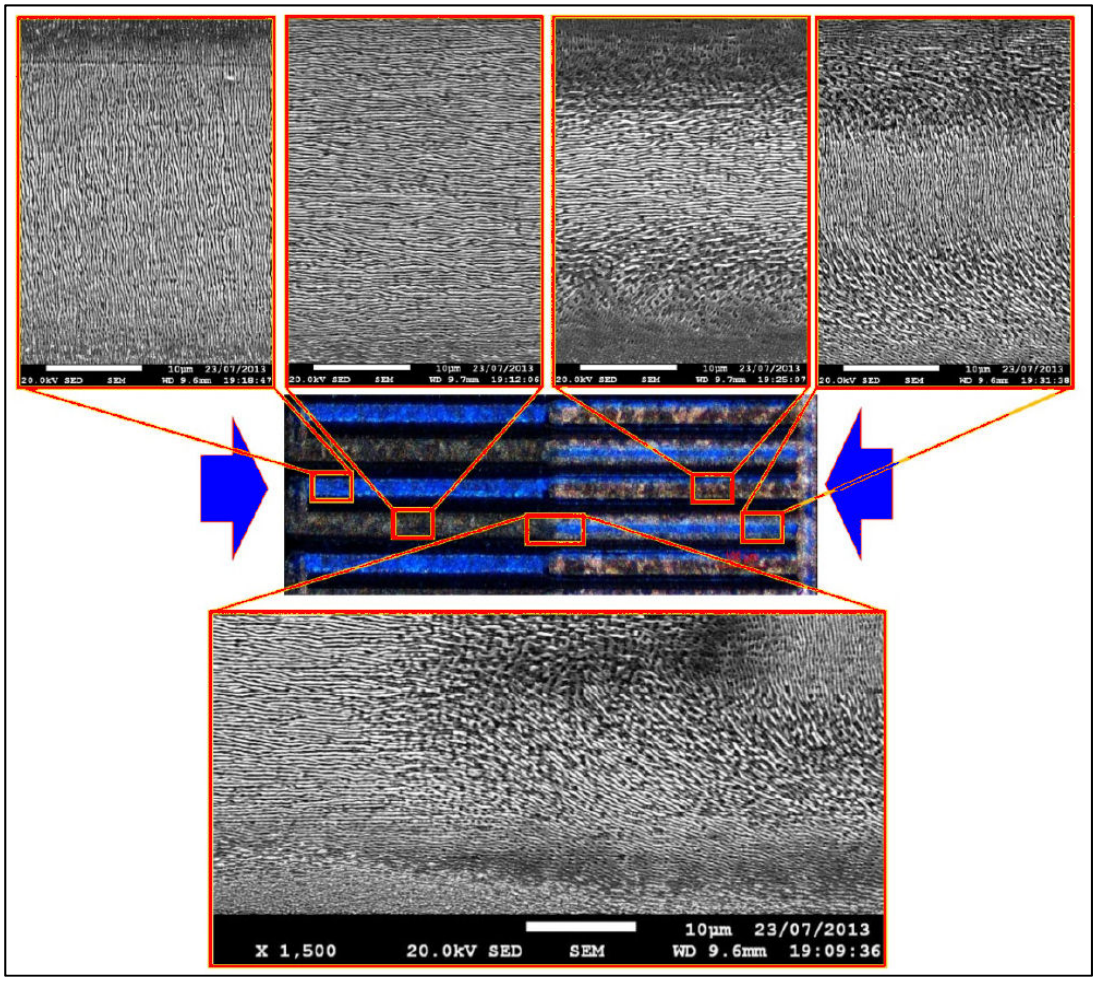

Fig. 3. (Centre) Optical micrograph showing the processed area, imaged with side-illumination at grazing incidence (blue arrows). Four states of polarization, linear horizontal and vertical, radial and azimuthal were sequentially produced to process each region within the scanning path. The magnified inlays (top and bottom) show SEM images of the complex patterns of LIPSS imprinted in each region.

4. Conclusions

Real-time modulation of spatially structured polarization fields has been demonstrated, using two phase-only SLMs combined with two waveplates and addressed dynamically to produce four distinct polarization states, sequentially swapped at a frequency of up to ν = 12.5 Hz. Radial and azimuthal as well as orthogonal linear polarization states were generated with high fidelity, all with a ring intensity distribution.

By synchronizing the SLMs with a Galvo micro-positioning system, complex, real-time surface nanostructuring was demonstrated on a polished metal sample. Arrays of desired polarization states and associated vector fields were confirmed unambiguously by observing LIPSS which are generated orthogonal to the local electric field vector components and further elucidated by the directional light diffraction from the LIPSS. Dynamic, real-time technique for fast polarization modulation with SLM's is demonstrated here for the first time and has great potential for industrial applications in both surface and volume micro and nano-structuring. Potential applications may, for example include complex security marking and the creation of photonic components (using high and low NA) via femtosecond inscription, including data storage. Efforts to increase the effective polarization switching bandwidth are now in progress.

References

R. Le Harzic, D. Breitling, M. Weikert, S. Sommer, C. Föhl, S. Valette, C. Donnet, E. Audouard, and F. Dausinger, "Pulse width and energy influence on laser micromachining of metals in a range of 100 fs to 5 ps," Appl. Surf. Sci. **249**(1-4), 322–331 (2005).

P. S. Banks, M. D. Feit, A. M. Rubenchik, B. C. Stuart, and M. D. Perry, "Material effects in ultra-short pulse laser drilling of metals," Appl. Phys., A Mater. Sci. Process. **69**(7), S377–S380 (1999).

D. Breitling, C. Föhl, F. Dausinger, T. Kononenko, and V. Konov, "Drilling of metals", in *Femtosecond Technology for Technical and Medical Applications,* Topics Appl. Phys. **96**, 131–156 (Springer-Verlag, 2004).

D. Breitling, A. Ruf, and F. Dausinger, "Fundamental aspects in machining of metals with short and ultrashort laser pulses," Proc. SPIE **5339**, 49–63 (2004).

N. Sudani, K. Venkatakrishnan, and B. Tan, “Laser singulation of thin wafer: die strength and surface roughness analysis of 80μm silicon dice,” Opt. Lasers Eng. **47**(7-8), 850–854 (2009).

G. Račiukaitis, S. Grubinskas, P. Gecys, and M. Gedvilas, “Selectiveness of laser processing due to energy coupling localization: case of thin film solar cell scribing,” Appl. Phys., A Mater. Sci. Process. **112**(1), 93–98 (2013).

D. Liu, Z. Kuang, W. Perrie, P. J. Scully, A. Baum, S. P. Edwardson, E. Fearon, G. Dearden, and K. G. Watkins, “High-speed uniform parallel 3D refractive index micro-structuring of poly(methyl methacrylate) for volume phase gratings,” Appl. Phys. B **101**(4), 817–823 (2010).

Y. Bellouard, A. Champion, B. Lenssen, M. Matteucci, A. Schaap, M. Beresna, C. Corbari, M. Gecevicius, P. Kazansky, O. Chappuis, M. Kral, R. Clavel, F. Barrot, J. M. Breguet, Y. Mabillard, S. Bottinelli, M. Hopper, C. Hoenninger, E. Mottay, and J. Lopez, “The Femtoprint Project,” JLMN **7**(1), 1–10 (2012).

M. Rioux, R. Tremblay, and P. A. Bélanger, “Linear, annular, and radial focusing with axicons and applications to laser machining,” Appl. Opt. **17**(10), 1532–1536 (1978).

N. Sanner, N. Huot, E. Audouard, C. Larat, and J. P. Huignard, “Direct ultrafast laser micro-structuring of materials using programmable beam shaping,” Opt. Lasers Eng. **45**(6), 737–741 (2007).

J. Hamazaki, R. Morita, K. Chujo, Y. Kobayashi, S. Tanda, and T. Omatsu, “Optical-vortex laser ablation,” Opt. Express **18**(3), 2144–2151 (2010).

M. Duocastella and C. B. Arnold, “Bessel and annular beams for materials processing,” Laser Photonics Rev. **6**(5), 607–621 (2012).

N. J. Jenness, K. D. Wulff, M. S. Johannes, M. J. Padgett, D. G. Cole, and R. L. Clark, “Three-dimensional parallel holographic micropatterning using a spatial light modulator,” Opt. Express **16**(20), 15942–15948 (2008).

Y. Hayasaki, T. Sugimoto, A. Takita, and N. Nishida, “Variable holographic femtosecond laser processing by use of a spatial light modulator,” Appl. Phys. Lett. **87**(3), 031101 (2005).

Z. Kuang, W. Perrie, D. Liu, S. Edwardson, J. Cheng, G. Dearden, and K. Watkins, “Diffractive multi-beam surface micro-processing using 10 ps laser pulses,” Appl. Surf. Sci. **255**(22), 9040–9044 (2009).

S. Hasegawa and Y. Hayasaki, “Polarization distribution control of parallel femtosecond pulses with spatial light modulators,” Opt. Express **21**(11), 12987–12995 (2013).

G. R. Fowles, *Introduction to Modern Optics* (Holt, Rinehart and Winston, Inc., New York, 1975), Chap. 2.

H. Kleinpoppen, *Constituents of Matter, Atoms, Molecules, Nuclei and Particles*, p142, Ed. Bergmann/Schaefer, Copyright Walter de Gruyer, Berlin, New York (1997), Berlin, Germany.

J. M. Guay, A. Villafranca, F. Baset, K. Popov, L. Ramunno, and V. R. Bhardwaj, “Polarization-dependent femtosecond laser ablation of poly-methyl methacrylate,” New J. Phys. **14**(8), 085010 (2012).

R. W. Boyd, *Nonlinear Optics* (Academic press, Burlington MA, Elsevier, 2008), Chap. 4.

A. Braun, G. Korn, X. Liu, D. Du, J. Squier, and G. Mourou, “Self-channeling of high-peak-power femtosecond laser pulses in air,” Opt. Lett. **20**(1), 73–75 (1995).

N. A. Panov, V. A. Makarov, V. Y. Fedorov, and O. G. Kosareva, “Filamentation of arbitrary polarized femtosecond laser pulses in case of high-order Kerr effect,” Opt. Lett. **38**(4), 537–539 (2013).

R. A. Fox, R. M. Kogan, and E. J. Robinson, “Laser Triple-Quantum Photoionization of Cesium,” Phys. Rev. Lett. **26**(23), 1416–1417 (1971).

R. M. Kogan, R. A. Fox, G. T. Burnham, and E. J. Robinson, “Two-photon ionization of cesium,” Bull. Am. Phys. Soc. **16**, 1411 (1971).

H. S. Carman and R. N. Compton, “High-order multiphoton ionization photoelectron spectroscopy of nitric oxide,” J. Chem. Phys. **90**(3), 1307 (1989).

D. D. Venable and R. B. Kay, “Polarization effects in four-photon conductivity in quartz,” Appl. Phys. Lett. **27**(1), 48–49 (1975).

V. V. Temnov, K. Sokolowski-Tinten, P. Zhou, A. El-Khamhawy, and D. von der Linde, “Multiphoton Ionization in Dielectrics: Comparison of Circular and Linear Polarization,” Phys. Rev. Lett. **97**(23), 237403 (2006).

H. R. Reiss, “Polarization Effects in High-Order Multiphoton Ionization,” Phys. Rev. Lett. **29**(17), 1129–1131
(1972).

17. O. J. Allegre, W. Perrie, K. Bauchert, D. Liu, S. P. Edwardson, G. Dearden, and K. G. Watkins, “Real-time control of polarisation in ultra-short-pulse laser micro-machining,” Appl. Phys., A Mater. Sci. Process. **107**(2), 445–454 (2012).

S. Nolte, C. Momma, G. Kamlage, A. Ostendorf, C. Fallnich, F. Von Alvensleben, and H. Welling, “Polarization effects in ultrashort-pulse laser drilling,” Appl. Phys., A Mater. Sci. Process. **68**(5), 563–567 (1999).

K. Venkatakrishnan, B. Tan, P. Stanley, and N. R. Sivakumar, “The effect of polarization on ultrashort pulsed laser ablation of thin metal films,” J. Appl. Phys. **92**(3), 1604–1607 (2002).

V. G. Niziev and A. V. Nesterov, “Influence of beam polarization on laser cutting efficiency,” J. Phys. D Appl. Phys. **32**(13), 1455–1461 (1999).

R. Weber, A. Michalowski, M. Abdou-Ahmed, V. Onuseit, V. Rominger, M. Kraus, and T. Graf, “Effects of radial and tangential polarization in laser material processing,” Phys. Procedia **12**, 21–30 (2011).

M. Meier, V. Romano, and T. Feurer, “Material processing with pulsed radially and azimuthally polarized laser radiation,” Appl. Phys., A Mater. Sci. Process. **86**(3), 329–334 (2007).

K. Venkatakrishnan and B. Tan, “Interconnect microvia drilling with a radially polarized laser beam,” J. Micromech. Microeng. **16**(12), 2603–2607 (2006).

M. R. Beversluis, L. Novotny, and S. J. Stranick, “Programmable vector point-spread function engineering,” Opt. Express 14(7), 2650–2656 (2006).

J. Qi, W. Sun, J. Liao, Y. Nie, X. Wang, J. Zhang, X. Liu, H. Jia, M. Lu, S. Chen, J. Liu, J. Yang, J. Tan, and X. Li, “Generation and analysis of both in-phase and out-phase radially polarized femtosecond-pulse beam,” Opt. Eng. 52(2), 024201 (2013).

O. J. Allegre, W. Perrie, S. P. Edwardson, G. Dearden, and K. G. Watkins, “Laser microprocessing of steel with radially and azimuthally polarized femtosecond vortex pulses,” J. Opt. 14(8), 085601 (2012).

O J Allegre, Y Jin,W Perrie, J Ouyang, E Fearon, S P Edwardson, G Dearden "Complete wavefront and polarization control for ultrashort-pulse laser microprocessing," OPTICS EXPRESS Vol. 21, No. 18 21198 (2013)

Y. Jin, O. J. Allegre, W. Perrie, K. Abrams, J. Ouyang, E. Fearon, S. P. Edwardson, G. Dearden. "Dynamic modulation of spatially structured polarization fields for real-time control of ultrafast laser-material interactions" OPTICS EXPRESS Vol. 21, No. 21 25333 (2013)